Fuzzy Approximation-Based Adaptive Finite-Time Tracking Control for a Quadrotor UAV with Actuator Faults

Wei Yang[1] · Guozeng Cui[1] · Ze Li[1] · Chongben Tao[1]

Abstract This article focuses on the problem of adaptive finite-time trajectory tracking control for a quadrotor unmanned aerial vehicle (UAV) with actuator faults. By introducing a novel finite-time command filter, the derivative of virtual control law is approximated, so the issue of "explosion of complexity" is successfully avoided. At the same time, the fractional power error compensation mechanism is constructed to quickly remove the effect of filtered error. By virtue of the command filter technique, backstepping design method, and event-triggered control strategy, the adaptive finite-time fault-tolerant controllers for a quadrotor UAV are designed. It is demonstrated that all signals of the closed-loop system are finite time bounded, and the attitude and position tracking errors can converge to a small neighborhood near the origin in a finite time. Finally, the simulation examples are given to validate the efficacy of the developed adaptive finite-time control algorithm.

Keywords Adaptive control · Fuzzy logic system · Finite-time control · Actuator faults · Quadrotor UAV

✉ Guozeng Cui
guozengcui@gmail.com

Wei Yang
yyw_78@163.com

Ze Li
lizeing@163.com

Chongben Tao
tom1tao@163.com

[1] School of Electronic and Information Engineering, Suzhou University of Science and Technology, Suzhou 215009, China

1 Introduction

In the past decades, trajectory tracking control of the quadrotor unmanned aerial vehicle (UAV) has been a hotspot due to its broad range of applications, including military defense, urban services, and plant protection [1–4]. A large number of studies have been reported on quadrotor UAVs via various control techniques, such as PID control [5], sliding mode control [6, 7], and backstepping control [8–10]. It should be noted that the chattering phenomenon in [6, 7] is inevitable and the drawback of "complexity explosion" in [8–10] also cannot be effectively solved.

Recently, a series of dynamic surface control (DSC) schemes have been presented for quadrotor UAVs in [11–13] to decrease the complexity of the existing control strategies. Meanwhile, the command filtered backstepping (CFB) technique was used for the trajectory tracking control of a quadrotor UAV [14], which eliminated unconsidered filtered errors [11–13] by introducing error compensating (EC) signals. In [15], an adaptive attitude loop controller via the CFB technique was constructed for a six-freedom nonlinear small UAV without precise models. Consider the quadrotor UAV with input saturation and disturbances, the command filter-based disturbance observer flight control algorithm was proposed in [16]. It is well known that fuzzy logic systems [17–20] and neural networks [21–23] are considered as powerful tools for controlling nonlinear systems owing to the universal approximation properties. Subsequently, some approximation-based adaptive control schemes for quadrotor UAVs [24–26] have been proposed, which effectively approximate the unknown nonlinear dynamics. However, the abovementioned control strategies are based on the premise that the control signals are continuously transmitted to

actuators, which occupy communication bandwidth and waste resources.

The event-triggered control (ETC) technique, which has the advantage of lower resource consumption, has been utilized to ease the communication burden of quadrotor UAVs. An event-triggered-based adaptive constraint control algorithm was proposed for a quadrotor UAV [27], which made the output errors meet the asymmetric constraints. Based on the fixed threshold ETC strategy in [28], the problem of tracking control for the quadrotor UAV was studied. When the quadrotor UAV raised external disturbances, an event-triggered-based adaptive controller was constructed in [29] to ensure the robustness of the closed-loop system. Given the quadrotor UAVs with input saturation, the antisaturation tracking control schemes in light of relative threshold ETC technique were proposed in [30, 31], respectively. Nevertheless, these results only guarantee asymptotic convergence. Finite-time control [32, 33] was considered to be the time-optimal control strategies with fast convergence and strong robustness. More recently, a series of finite-time flight control algorithms for quadrotor UAVs have been presented, see, e.g., [34–38], which have superiorities in convergence speed and robustness. In [34], the problem of finite-time formation control for quadrotor UAVs was investigated. For the attitude system, the adaptive flight controllers were designed in [35, 36] based on the finite-time stability theory. In the cases of input saturation and model uncertainties, the adaptive finite-time control strategies were developed in [37, 38], which guaranteed the global convergence of quadrotor UAVs.

On the other hand, the unexpected failures on the quadrotor UAV could severely degrade the flight performance and even lead to the crash, so it is essential to guarantee the fault tolerance of the flight controller. In [39], the complete fault of the single rotor for the quadrotor UAV was considered. The controllability remained at the expense of rolling angle freedom, which means that the UAV cannot complete the established task but to make a forced landing. Using sliding mode control and observer technique, the fault-tolerant control strategies for quadrotor UAVs were proposed in [40, 41], respectively. In [42], the distributed finite-time containment controller for multi-UAVs with actuator faults was designed using the minimum learning parameter technique. The problem of adaptive finite-time fault-tolerant control for single UAV [43] was considered, and the distributed finite-time control algorithm for multi-UAVs [44] with actuator faults was

proposed. To the best of author's knowledge, the event-triggered-based adaptive finite-time trajectory tracking control for quadrotor UAVs with actuator faults via CFB technique has not been solved.

Inspired by the preceding discussion, this article investigates the problem of trajectory tracking control for a quadrotor UAV with actuator faults and develops a fuzzy approximation-based event-triggered adaptive finite-time fault-tolerant control strategy. The main contributions of this article are summarized as follows:

(1) The proposed finite-time command filtered back-stepping (FTCFB) control strategy, by combining the finite-time command filter technique and the fractional power error compensation mechanism, not only overcomes the issue of "explosion of complexity" in [8–10] but also eliminates the effect of filtered error unsettled in DSC [11–13], resulting in faster convergence and better tracking performance.

(2) Different from the asymptotical convergence control schemes for quadrotor UAVs [14–16] related to CFB technique, the ETC algorithm based on the relative thresholds event-triggered mechanism is developed, which reduces the execution number of actuators while saving the computing resources of the airborne platform. In addition, the attitude and position tracking errors can converge to a small neighborhood near the origin in a finite time.

(3) In contrast to the existing fault-tolerant control schemes [39–41], the partial loss of effectiveness and unknown bias faults in actuators are both considered in this paper. Especially, the prior information of bias faults is no longer required based on the adaptive compensation technique.

The rest of this paper is organized as follows. The model description and preliminaries are provided in Sect. 2. In Sect. 3, the finite-time fault-tolerant control scheme for the quadrotor UAV is developed and the stability analysis is also provided. The simulation results and the conclusion are presented in Sects. 4 and 5, respectively.

2 Model Description and Preliminaries

2.1 Model Description

Consider the quadrotor UAV and its dynamics model is described as follows:

$$\begin{cases} \ddot{\phi} = \dfrac{a}{I_x}\tau_\phi + \dfrac{I_y - I_z}{I_x}\dot{\theta}\dot{\psi} + \dfrac{J_r}{I_x}\varpi_r\dot{\theta} + d_\phi \\[2mm] \ddot{\theta} = \dfrac{a}{I_y}\tau_\theta + \dfrac{I_z - I_x}{I_y}\dot{\phi}\dot{\psi} - \dfrac{J_r}{I_y}\varpi_r\dot{\phi} + d_\theta \\[2mm] \ddot{\psi} = \dfrac{1}{I_z}\tau_\psi + \dfrac{I_x - I_y}{I_z}\dot{\phi}\dot{\theta} + d_\psi \\[2mm] \ddot{z} = \dfrac{1}{m}\tau_T(\cos\phi\cos\theta) - g + d_z \\[2mm] \ddot{x} = \dfrac{1}{m}\tau_T(\cos\phi\sin\theta\cos\psi + \sin\phi\sin\psi) + d_x \\[2mm] \ddot{y} = \dfrac{1}{m}\tau_T(\cos\phi\sin\theta\sin\psi - \sin\phi\cos\psi) + d_y \end{cases} \quad , \quad (1)$$

where ϕ, θ, ψ represent roll, pitch, and yaw angle; the positions of quadrotor UAV in space are described by x, y, and z. g is the gravitational acceleration. m and a indicate the mass of UAV and the distance from the fuselage center to the propeller shaft; I_x, I_y, I_z stand for the moment inertia of UAV; J_r and ϖ_r denote the moment inertia and angular speeds of the rotors. For $i = \phi, \theta, \psi, z, x, y$, d_i denotes bounded disturbance satisfying $|d_i| \le \bar{d}_i$ with $\bar{d}_i > 0$ being a constant. $\tau_\phi, \tau_\theta, \tau_\psi$ and τ_T are control inputs.

The actuator fault model of quadrotor UAV can be formulated as [45]: $u_i^f = \rho_i u_i^a + b_i$, where $\rho_i \in (0, 1]$ indicates the residual efficiency factor; b_i is the unknown time-varying bias fault; and u_i^a is the actual control input signal. Define $(\eta_1, \eta_2, \eta_3, \eta_4, \eta_5, \eta_6) = (\phi, \theta, \psi, z, x, y)$, and the dynamics model of quadrotor UAV can be rewritten as

$$\ddot{\eta}_i = g_i(\rho_i u_i^a + b_i) + f_i + d_i, \quad i = 1, 2, 3 \quad (2)$$

$$\ddot{\eta}_i = g_i(\rho_i u_i^a + b_i) + d_i, \quad i = 4, 5, 6, \quad (3)$$

where $(g_1, g_2, g_3) = (a/I_x, a/I_y, 1/I_z)$, $g_4 = g_5 = g_6 = 1/m$, $(u_1^f, u_2^f, u_3^f) = (\tau_\phi, \tau_\theta, \tau_\psi)$, $(u_4^f, u_5^f, u_6^f) = (\tau_T(\cos\phi\cos\theta) - mg, \tau_T(\cos\phi\sin\theta\cos\psi + \sin\phi\sin\psi)$, $\tau_T(\cos\phi\sin\theta\sin\psi - \sin\phi\cos\psi))$, $(f_1, f_2, f_3) = (\dot{\theta}\dot{\psi}(I_y - I_z)/I_x + \varpi_r\dot{\theta}J_r/I_x, \dot{\phi}\dot{\psi}(I_z - I_x)/I_y - \varpi_r\dot{\phi}J_r/I_y, \dot{\phi}\dot{\theta}(I_x - I_y)/I_z)$, $(d_1, d_2, d_3) = (d_\phi, d_\theta, d_\psi)$, and $(d_4, d_5, d_6) = (d_z, d_x, d_y)$.

The control goal of this article is to design an event-triggered-based adaptive finite-time fault-tolerant control scheme for a quadrotor UAV, which ensures the position and attitude outputs quickly track the reference trajectories in a finite time and guarantees the finite-time boundedness of all closed-loop system signals.

Assumption 1 For $i = 3, 4, 5, 6$, the reference trajectories η_i^d and its first-order derivative $\dot{\eta}_i^d$ are continuous and bounded.

2.2 Fuzzy Logic System

Fuzzy logic system uses fuzzy If-then rules to realize the mapping from input vector $x = [x_1, x_2, \ldots, x_n]^\top$ to output variable $y \in U$, and the lth If-then rule can be indicated as: $R^l :$. For $l = 1, \ldots, N$, if $x_1 = F_1^l$, $x_2 = F_2^l, \ldots,$ and $x_n = F_n^l$, then $y = G^l$, where F_i^l and G^l are fuzzy sets corresponding to fuzzy membership functions $\mu_{F_i^l}(x_i)$ and $\mu_{G^l}(y)$, and N is the number of fuzzy rules. If the methods of single-point fuzzification, product reasoning, and center-weighted defuzzification are adopted, the fuzzy logic system can be expressed as $y(x) = \sum_{l=1}^N \bar{y}_l \prod_{i=1}^n \mu_{F_i^l}(x_i) / \sum_{l=1}^N \prod_{i=1}^n \mu_{F_i^l}(x_i)$, where $\bar{y}_l = \max_{y \in U} \mu_{G^l}(y)$. The following fuzzy basis functions are defined as $\varphi_l = \prod_{i=1}^n \mu_{F_i^l}(x_i) / \sum_{l=1}^N \prod_{i=1}^n \mu_{F_i^l}(x_i)$. Let $\Xi = [\bar{y}_1, \bar{y}_2, \ldots, \bar{y}_N]^\top = [\Xi_1, \Xi_2, \ldots, \Xi_N]^\top$ and $\varphi^\top(x) = [\varphi_1(x), \varphi_2(x), \ldots, \varphi_N(x)]$, then the fuzzy logic system can be expressed as $y(x) = \Xi^\top \varphi(x)$.

Lemma 1 ([46]) *Assume that $f(x)$ is a continuous function defined on the compact set Ω, for any given constant $\bar{\omega} > 0$, there exists a fuzzy logic system such that*

$$\sup_{x \in \Omega} |f(x) - \Xi^\top \varphi(x)| \le \bar{\omega}.$$

2.3 Finite-Time Control

Definition 1 ([47]) *For the nonlinear system $\dot{\Upsilon} = \beth(\Upsilon)$ with the initial condition $\Upsilon(t_0) = \Upsilon_0$, if there exist a positive constant $\hbar$ and the setting time $t^*(\hbar, \Upsilon_0)$ to make $\|\Upsilon(t)\| < \hbar$ for all $t > t_0 + t^*$, then the equilibrium $\Upsilon = 0$ of the nonlinear system $\dot{\Upsilon} = \beth(\Upsilon)$ is semi-global practical finite-time stable.*

Lemma 2 ([48]) *For the given scalars $0 < \mathfrak{n} < 1$, $\mathfrak{w}_1 > 0$, $\mathfrak{w}_2 > 0$, and $0 < \mathfrak{w}_3 < \infty$, if there exists a continuous positive definite function $Ł(\Upsilon)$ in relation to the nonlinear system $\dot{\Upsilon} = \beth(\Upsilon)$ such that $\dot{Ł}(\Upsilon) \le -\mathfrak{w}_1 Ł(\Upsilon) - \mathfrak{w}_2 Ł(\Upsilon)^\mathfrak{n} + \mathfrak{w}_3$, then the solution of $\dot{\Upsilon} = \beth(\Upsilon)$ is semi-global practical finite-time stable, where the upper bound of the setting time t^* is $t^* \le \max\{t_0 + \frac{1}{\pi_0 \mathfrak{w}_1(1-\mathfrak{n})} \ln \frac{\pi_0 \mathfrak{w}_1 Ł^{1-\mathfrak{n}}(t_0) + \mathfrak{w}_2}{\mathfrak{w}_2}, t_0 + \frac{1}{\mathfrak{w}_1(1-\mathfrak{n})} \ln \frac{\mathfrak{w}_1 Ł^{1-\mathfrak{n}}(t_0) + \pi_0 \mathfrak{w}_2}{\pi_0 \mathfrak{w}_2}\}$, and π_0 satisfies $0 < \pi_0 < 1$.*

2.4 Useful Lemmas

Lemma 3 ([49]) *Suppose that* $\beth(\mathcal{P}, \mathcal{Q}) > 0$ *stands for a real-valued function, and A and B are the constants greater than zero, and one has*

$$\mid \mathcal{P} \mid^A \mid \mathcal{Q} \mid^B \leq \frac{A}{A+B} \beth(\mathcal{P}, \mathcal{Q}) \mid \mathcal{P} \mid^{A+B}$$
$$+ \frac{B}{A+B} \beth(\mathcal{P}, \mathcal{Q})^{-\frac{A}{B}} \mid \mathcal{Q} \mid^{A+B} .$$

Lemma 4 ([50]) *For* $p = 1, \cdots, q$, $0 < \mathcal{G} \leq 1$, *and* $\mathcal{T}_p \in \mathbb{R}$, *the following inequality can be obtained*

$$\left(\sum_{p=1}^{q} \mid \mathcal{T}_p \mid \right)^{\mathcal{G}} \leq \sum_{p=1}^{q} \mid \mathcal{T}_p \mid^{\mathcal{G}} \leq q^{1-\mathcal{G}} \left(\sum_{p=1}^{q} \mid \mathcal{T}_p \mid \right)^{\mathcal{G}} .$$

3 Finite-Time Fault-Tolerant Controller Design

In this section, the adaptive finite-time fault-tolerant control scheme for attitude subsystem and position subsystem of the quadrotor UAV is presented based on the event-triggered mechanism and CFB design method, respectively.

3.1 Controller Design for Attitude Subsystem

Defining the tracking errors as $\upsilon_{i,1} = \eta_i - \eta_i^d$ and $\upsilon_{i,2} = \dot{\eta}_i - \alpha_{i,1}^c$. $\zeta_{i,1} = \upsilon_{i,1} - z_{i,1}$ and $\zeta_{i,2} = \upsilon_{i,2} - z_{i,2}$ are the compensated tracking errors, $i = 1, 2, 3$, where η_i^d denotes the reference trajectory; $z_{i,1}, z_{i,2}$ are EC signals which will be given later. $\alpha_{i,1}^c$ is the filter output with the virtual control law $\alpha_{i,1}$ as input, where the following finite-time command filter [51] is adopted:

$$\begin{cases} \dot{\epsilon}_{i,1} = \epsilon_{i,2} \\ \dot{\epsilon}_{i,2} = \frac{1}{\mathfrak{R}_i^2} \left(-\mathfrak{L}_{i,1} \arctan\left(\epsilon_{i,1} - \alpha_{i,1}\right) - \mathfrak{L}_{i,2} \arctan\left(\mathfrak{R}_i \epsilon_{i,2}\right)\right) \end{cases} , \tag{4}$$

where $\mathfrak{R}_i$, $\mathfrak{L}_{i,1}$, and $\mathfrak{L}_{i,2}$ are positive constants, $\epsilon_{i,1} = \alpha_{i,1}^c$ and $\epsilon_{i,2} = \dot{\alpha}_{i,1}^c$.

The virtual control law $\alpha_{i,1}$ and EC signal $z_{i,1}$ are designed as

$$\alpha_{i,1} = -\mathfrak{p}_{i,1} \upsilon_{i,1} + \dot{\eta}_i^d - \mathfrak{q}_{i,1} \zeta_{i,1}^{\mathfrak{n}} \tag{5}$$

$$\dot{z}_{i,1} = -\mathfrak{p}_{i,1} z_{i,1} + z_{i,2} + \left(\alpha_{i,1}^c - \alpha_{i,1}\right) - \mathfrak{r}_{i,1} z_{i,1}^{\mathfrak{n}} , \tag{6}$$

where $\mathfrak{p}_{i,1}$, $\mathfrak{q}_{i,1}$, and $\mathfrak{r}_{i,1}$ are positive design constants; $1/2 < \mathfrak{n} = \mathfrak{n}_1/\mathfrak{n}_2 < 1$, $\mathfrak{n}_1$, and $\mathfrak{n}_2$ are positive odd integers. From (5) and (6), the time derivative of $\zeta_{i,1}$ is computed as

$$\dot{\zeta}_{i,1} = \zeta_{i,2} - \mathfrak{p}_{i,1} \zeta_{i,1} - \mathfrak{q}_{i,1} \zeta_{i,1}^{\mathfrak{n}} + \mathfrak{r}_{i,1} z_{i,1}^{\mathfrak{n}} . \tag{7}$$

Remark 1 Note that the conventional backstepping control schemes for the quadrotor UAV [8–10] require repeated derivation of the virtual control law, which result in the issue of "explosion of complexity". In this paper, the finite-time command filter is introduced to quickly obtain $\alpha_{i,1}^c$ and $\dot{\alpha}_{i,1}^c$ to replace $\alpha_{i,1}$ and its derivative $\dot{\alpha}_{i,1}$, thus reducing the computational complexity of the proposed control algorithm.

Differentiating $\zeta_{i,2}$ together with (2) yields

$$\dot{\zeta}_{i,2} = g_i \rho_i u_i^a + g_i b_i + f_i + d_i - \dot{\alpha}_{i,1}^c - \dot{z}_{i,2} . \tag{8}$$

From Lemma 1, the fuzzy logic system can be utilized to approximate the unknown nonlinear function $f_i = \Xi_i^{*\top} \varphi_i + \omega_i$, $\mid \omega_i \mid \leq \bar{\omega}_i$, where $\bar{\omega}_i$ is a positive constant; Ξ_i^* is the weight vector. $\hat{\Gamma}_i$ is the estimation of the unknown constant, $\Gamma_i = \|\Xi_i^*\|^2$, and $\tilde{\Gamma}_i = \Gamma_i - \hat{\Gamma}_i$ is the estimation error. Using Lemma 3, one has

$$\zeta_{i,2} d_i \leq \frac{1}{2} \zeta_{i,2}^2 + \frac{1}{2} \bar{d}_i^2 \tag{9}$$

$$\zeta_{i,2} f_i \leq \frac{\zeta_{i,2}^2 \|\Xi_i^*\|^2 \varphi_i^\top \varphi_i}{2\mathfrak{h}_i^2} + \frac{1}{2} \mathfrak{h}_i^2 + \frac{1}{2} \zeta_{i,2}^2 + \frac{1}{2} \bar{\omega}_i^2 , \tag{10}$$

where $\mathfrak{h}_i > 0$ is a constant. Define $\Lambda_i = b_i$, and $\tilde{\Lambda}_i = \Lambda_i - \hat{\Lambda}_i$ is the estimation error. The virtual control law $\alpha_{i,2}$ and EC signal $z_{i,2}$ are given as

$$\alpha_{i,2} = \frac{1}{g_i \rho_i} \left(\mathfrak{p}_{i,} \upsilon_{i,} + \mathfrak{q}_{i,} \zeta_{i,}^{\mathfrak{n}} + \upsilon_{i,} - \alpha_{i,}^{\epsilon} + \zeta_{i,} \right.$$
$$\left. + \frac{\zeta_{i,2} \hat{\Gamma}_i \varphi_i^\top \varphi_i}{2\mathfrak{h}_{i}} + g_i \hat{\Lambda}_i \right) \tag{11}$$

$$\dot{z}_{i,2} = -\mathfrak{p}_{i,2} z_{i,2} - z_{i,1} - \mathfrak{r}_{i,2} z_{i,2}^{\mathfrak{n}} , \tag{12}$$

where $\mathfrak{p}_{i,2}$, $\mathfrak{q}_{i,2}$, and $\mathfrak{r}_{i,2}$ are positive design parameters. The parameter tuning laws $\hat{\Lambda}_i$ and $\hat{\Gamma}_i$ are selected as

$$\dot{\hat{\Lambda}}_i = \mathfrak{k}_{i,1} g_i \zeta_{i,2} - \mathfrak{l}_{i,1} \hat{\Lambda}_i \tag{13}$$

$$\dot{\hat{\Gamma}}_i = \mathfrak{k}_{i,2} \frac{\zeta_{i,2}^2 \varphi_i^\top \varphi_i}{2\mathfrak{h}_i^2} - \mathfrak{l}_{i,2} \hat{\Gamma}_i , \tag{14}$$

where $\mathfrak{k}_{i,j} > 0$ and $\mathfrak{l}_{i,j} > 0$ are constants.

In light of ETC strategy, the intermediate control law β_i is designed as

$$\beta_i(t) = -(1 + \mu_i)\left(\alpha_{i,2} \tanh\left(\frac{\zeta_{i,2}\alpha_{i,2}}{\kappa_i}\right) + \varsigma_{i,1} \tanh\left(\frac{\zeta_{i,2}\varsigma_{i,1}}{\kappa_i}\right)\right),$$

$$(15)$$

where $0 < \mu_i < 1$ and $\kappa_i > 0$. For all $t \in [t_{k,i}, t_{k+1,i})$, $u_i^a(t) = \beta_i(t_{k,i})$ indicates the actual control law. Define $e_i(t) = \beta_i(t) - u_i^a(t)$ and construct the event-triggered mechanism as

$$t_{k+1,i} = \inf\left\{ \mathfrak{t} \in \mathbb{R} \mid | e_i(t) | \geq \mu_i | u_i^a(t) | + \varsigma_{i,2} \right\}, \quad (16)$$

where $\varsigma_{i,1}$ and $\varsigma_{i,2}$ are design parameters satisfying $\varsigma_{i,1} > \varsigma_{i,2}/(1 - \mu_i)$. $t_{k,i}, k \in \mathbb{Z}^+$, is the label of update moment. When (16) is satisfied, t is labeled as $t_{k+1,i}$ and the intermediate control law $\beta_i(t_{k+1,i})$ is transmitted to the actual control law $u_i^a(t)$, otherwise $u_i^a(t)$ remains the constant $\beta_i(t_{k,i})$ until the next triggered moment. Using (16), $u_i^a(t)$ can be alternated by

$$u_i^a(t) = \frac{\beta_i(t)}{1 + \Phi_{i,1}(t)\mu_i} - \frac{\Phi_{i,2}(t)\varsigma_{i,2}}{1 + \Phi_{i,1}(t)\mu_i} \quad (17)$$

with $| \Phi_{i,1}(t) | \leq 1$ and $| \Phi_{i,2}(t) | \leq 1$ being continuous time-varying functions.

3.2 Controller Design for Position Subsystem

Define $v_{i,1} = \eta_i - \eta_i^d$, $v_{i,2} = \dot{\eta}_i - \alpha_{i,1}^c$, $i = 4, 5, 6$, as the tracking errors, where η_i^d represents the reference trajectory; $\alpha_{i,1}$ is the virtual control law; and $\alpha_{i,1}^c = \epsilon_{i,1}$ and $\dot{\alpha}_{i,1}^c = \epsilon_{i,2}$. Define the compensated tracking errors as $\zeta_{i,1} = v_{i,1} - z_{i,1}$, $\zeta_{i,2} = v_{i,2} - z_{i,2}$ with $z_{i,1}, z_{i,2}$ being EC signals.

Design the virtual control law $\alpha_{i,1}$ and EC signal $z_{i,1}$ as

$$\alpha_{i,1} = -\mathfrak{p}_{i,1} v_{i,1} + \dot{\eta}_i^d - \mathfrak{q}_{i,1} \zeta_{i,1}^\mathfrak{n} \quad (18)$$

$$\dot{z}_{i,1} = -\mathfrak{p}_{i,1} z_{i,1} + z_{i,2} + \left(\alpha_{i,1}^c - \alpha_{i,1}\right) - \mathfrak{r}_{i,1} z_{i,1}^\mathfrak{n}, \quad (19)$$

where $\mathfrak{p}_{i,1}$, $\mathfrak{q}_{i,1}$, and $\mathfrak{r}_{i,1}$ are positive design parameters. Using (18) and (19), $\dot{\zeta}_{i,1}$ is computed as

$$\dot{\zeta}_{i,1} = \zeta_{i,2} - \mathfrak{p}_{i,1} \zeta_{i,1} - \mathfrak{q}_{i,1} \zeta_{i,1}^\mathfrak{n} + \mathfrak{r}_{i,1} z_{i,1}^\mathfrak{n}. \quad (20)$$

According to (3), the time derivative of $z_{i,2}$ can be obtained as

$$\dot{\zeta}_{i,2} = g_i \rho_i u_i^a + g_i b_i + d_i - \dot{\alpha}_{i,1}^c - \dot{z}_{i,2}. \quad (21)$$

The virtual control law $\alpha_{i,2}$ and EC signal $z_{i,2}$ are constructed as

$$\alpha_{i,2} = \frac{1}{g_i \rho_i}\left(\mathfrak{p}_{i,} v_{i,} + \mathfrak{q}_{i,} \zeta_{i,}^\mathfrak{n} + v_{i,} - \alpha_{i,}^{\mathfrak{c}} + \zeta_{i,} + g_i \Lambda_i\right) \quad (22)$$

$$\dot{z}_{i,2} = -\mathfrak{p}_{i,2} z_{i,2} - z_{i,1} - \mathfrak{r}_{i,2} z_{i,2}^\mathfrak{n}, \quad (23)$$

where $\mathfrak{p}_{i,2}$, $\mathfrak{q}_{i,2}$, and $\mathfrak{r}_{i,2}$ are positive constants. $\Lambda_i = b_i$; $\hat{\Lambda}_i$ is the estimation of Λ_i and $\tilde{\Lambda}_i = \Lambda_i - \hat{\Lambda}_i$. The parameter tuning law $\hat{\Lambda}_i$ is consequently chosen as

$$\dot{\hat{\Lambda}}_i = \mathfrak{k}_{i,1} g_i \zeta_{i,2} - \mathfrak{l}_{i,1} \hat{\Lambda}_i \quad (24)$$

with $\mathfrak{k}_{i,1}$ and $\mathfrak{l}_{i,1}$ being positive design parameters.

By applying the ETC approach to the position subsystem (3), the intermediate control law β_i is given as

$$\beta_i(t) = -(1 + \mu_i)\left(\alpha_{i,2} \tanh\left(\frac{\zeta_{i,2}\alpha_{i,2}}{\kappa_i}\right) + \varsigma_{i,1} \tanh\left(\frac{\zeta_{i,2}\varsigma_{i,1}}{\kappa_i}\right)\right),$$

$$(25)$$

where $0 < \mu_i < 1$ and $\kappa_i > 0$. The actual control law u_i^a and the event-triggered mechanism are given by

$$u_i^a(t) = \beta_i(t_{k,i}), \quad \forall t \in [t_{k,i}, t_{k+1,i}) \quad (26)$$

$$t_{k+1,i} = \inf\left\{ \mathfrak{t} \in \mathbb{R} \mid | e_i(t) | \geq \mu_i | u_i^a(t) | + \varsigma_{i,2} \right\}, \quad (27)$$

where $e_i(t) = \beta_i(t) - u_i^a(t)$, $\varsigma_{i,1} > \varsigma_{i,2}/(1 - \mu_i)$, and $\varsigma_{i,2} > 0$. $t_{k,i}, k \in \mathbb{Z}^+$, is the controller update time. If $t \in [t_{k,i}, t_{k+1,i})$, the actual control law $u_i^a(t)$ remains a constant $\beta_i(t_{k,i})$; when the event-triggered mechanism (27) is triggered, the time instant is noted as $t_{k+1,i}$ and the intermediate control law $\beta_i(t_{k+1,i})$ is applied to $u_i^a(t)$. Moreover, on the basis of (27), one yields

$$u_i^a(t) = \frac{\beta_i(t)}{1 + \Phi_{i,1}(t)\mu_i} - \frac{\Phi_{i,2}(t)\varsigma_{i,2}}{1 + \Phi_{i,1}(t)\mu_i}, \quad (28)$$

where $| \Phi_{i,1}(t) | \leq 1$ and $| \Phi_{i,2}(t) | \leq 1$ are continuous time-varying functions.

Based on the coupling among the total lift force τ_T, the reference trajectories of roll angle η_1^d and pitch angle η_2^d, the control inputs of position subsystem u_4^f, u_5^f, u_6^f, and the yaw angle η_3, the following equalities can be obtained

$$\tau_T = \sqrt{(u_4^f + mg)^2 + (u_5^f)^2 + (u_6^f)^2}$$

$$\eta_1^d = \arcsin\left(\frac{u_5^f \sin \eta_3 - u_6^f \cos \eta_3}{\tau_T}\right)$$

$$\eta_2^d = \arctan\left(\frac{u_5^f \cos \eta_3 + u_6^f \sin \eta_3}{u_4^f + mg}\right).$$

In summary, the above fuzzy approximation-based event-triggered adaptive finite-time fault-tolerant control design procedures for the quadrotor UAV is presented in Fig. 1.
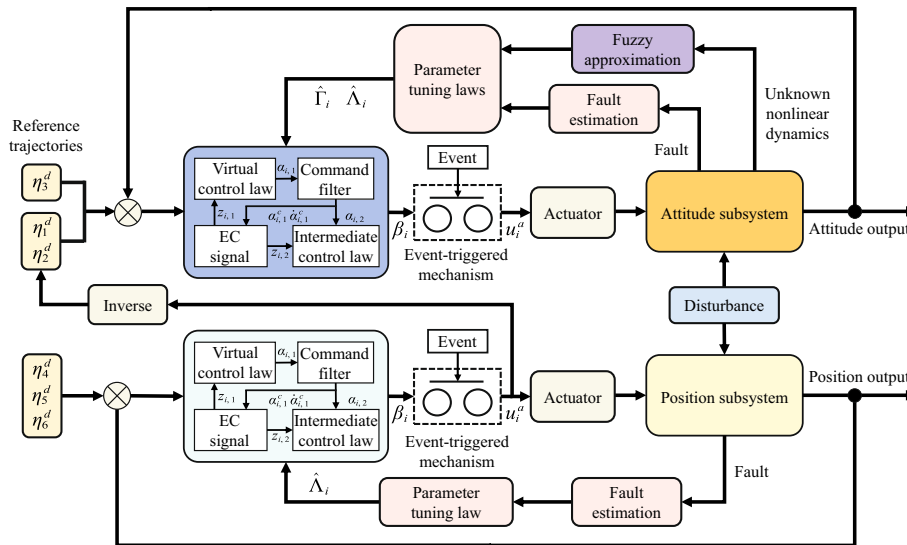
Fig. 1 The fuzzy approximation-based event-triggered adaptive finite-time fault-tolerant control block diagram

4 Stability Analysis

Theorem 1 *Consider the quadrotor UAV* (1) *under Assumption* 1, *the event-triggered adaptive finite-time fault-tolerant control scheme, including the control laws* (5), (11), (18), (22), *the EC signals* (6), (12), (19), (23), *and the parameter tuning laws* (13), (14), (24) *ensures that the attitude and position tracking errors converge to a sufficient neighborhood around origin in a finite time, while all signals of the attitude and position subsystems are finite-time bounded.*

Proof The detailed proof for the Theorem 1 is given as follows:

Step 1: Select the Lyapunov function as $V_1 = \frac{1}{2}\sum_{i=1}^{6}\left(\zeta_{i,1}^2 + z_{i,1}^2\right)$. The time derivative of V_1 together with (6), (7), (19), and (20) is calculated as

$$\dot{V}_1 = \sum_{i=1}^{6}\left\{-\mathfrak{p}_{i,1}\zeta_{i,1}^2 - \mathfrak{q}_{i,1}\zeta_{i,1}^{1+\mathfrak{n}} + \mathfrak{r}_{i,1}\zeta_{i,1}z_{i,1}^{\mathfrak{n}} + \zeta_{i,1}\zeta_{i,2} + z_{i,1}z_{i,2}\right.$$
$$\left. - \mathfrak{p}_{i,1}z_{i,1}^2 - \mathfrak{r}_{i,1}z_{i,1}^{1+\mathfrak{n}} + z_{i,1}\left(\alpha_{i,1}^c - \alpha_{i,1}\right)\right\}.$$

$$(29)$$

Step 2: Consider the Lyapunov function $V_2 = V_1 + \frac{1}{2}\sum_{i=1}^{6}\left(\zeta_{i,2}^2 + z_{i,2}^2 + \frac{1}{\mathfrak{t}_{i,1}}\tilde{\Lambda}_i^2\right) + \sum_{i=1}^{3}\frac{1}{2\mathfrak{t}_{i,2}}\tilde{\Gamma}_i^2$. From (8) and (21), the time derivative of V_2 is given as

$$\dot{V}_2 = \dot{V}_1 + \sum_{i=1}^{6}\left\{\zeta_{i,2}g_i\rho_i u_i^a + \zeta_{i,2}\left(g_i\Lambda_i + d_i - \dot{\alpha}_{i,1}^c - \dot{z}_{i,2}\right)\right.$$
$$\left. + z_{i,2}\dot{z}_{i,2} - \frac{1}{\mathfrak{t}_{i,1}}\tilde{\Lambda}_i\dot{\hat{\Lambda}}_i\right\} + \sum_{i=1}^{3}\left\{\zeta_{i,2}f_i - \frac{1}{\mathfrak{t}_{i,2}}\tilde{\Gamma}_i\dot{\hat{\Gamma}}_i\right\}.$$

$$(30)$$

Invoking (9), (10), (15), (17), (25), and (28) into (30) results in

$$\dot{V}_2 \leq \dot{V}_1 - \sum_{i=1}^{6}\left\{\zeta_{i,2}\left(g_i\rho_i\alpha_{i,2} - g_i\Lambda_i - \frac{1}{2}\zeta_{i,2} + \dot{\alpha}_{i,1}^c + \dot{z}_{i,2}\right) - z_{i,2}\dot{z}_{i,2}\right\}$$
$$+ \sum_{i=1}^{3}\left\{\frac{1}{2}\zeta_{i,1}^2 - \frac{1}{\mathfrak{t}_{i,2}}\tilde{\Gamma}_i\dot{\hat{\Gamma}}_i + \zeta_{i,2}^2\frac{\|\Xi_i^*\|^2\varphi_i^\top\varphi_i}{2\mathfrak{b}_i^2}\right\}$$
$$+ \sum_{i=1}^{6}g_i\rho_i\left\{|\zeta_{i,2}\alpha_{i,2}|\right.$$
$$\left. -\zeta_{i,2}\alpha_{i,2}\tanh\left(\frac{\zeta_{i,2}\alpha_{i,2}}{\kappa_i}\right) + |\zeta_{i,2}\varsigma_{i,1}| - \zeta_{i,2}\varsigma_{i,1}\tanh\left(\frac{\zeta_{i,2}\varsigma_{i,1}}{\kappa_i}\right)\right\}$$
$$- \sum_{i=1}^{6}\frac{1}{\mathfrak{t}_{i,1}}\tilde{\Lambda}_i\dot{\hat{\Lambda}}_i + \frac{1}{2}\sum_{i=1}^{6}\bar{d}_i^2 + \frac{1}{2}\sum_{i=1}^{3}\left(\mathfrak{h}_i^2 + \bar{\omega}_i^2\right).$$

$$(31)$$

Based on [, Theorem 1], one has $52|\alpha_{i,1}^c - \alpha_{i,1}| = \mathfrak{O}_i(\delta_i^{\iota\sigma})$, where ι and σ are positive constants and $\mathfrak{O}_i(\delta_i^{\iota\sigma})$ is the $\delta_i^{\iota\sigma}$ order approximation error. Furthermore, the following inequality holds

$$z_{i,1}\left(\alpha_{i,1}^c - \alpha_{i,1}\right) \leq |z_{i,1}||\alpha_{i,1}^c - \alpha_{i,1}| \leq \frac{1}{2}\mathfrak{O}_i\left(\delta_i^{2\iota\sigma}\right) + \frac{1}{2}z_{i,1}^2.$$

$$(32)$$

From (11)–(14), (22)–(24), and (29), (32) and on the basis of the inequality that $0 \leq |\vartheta| - \vartheta\tanh(\vartheta/\kappa_i) \leq 0.2785\kappa_i$, it follows that

$$\dot{V}_2 \leq \sum_{i=1}^{6}\left\{-\mathfrak{p}_{i,1}\zeta_{i,1}^2-(\mathfrak{p}_{i,1}-\frac{1}{2})z_{i,1}^2-\mathfrak{p}_{i,2}\zeta_{i,2}^2-\mathfrak{p}_{i,2}z_{i,2}^2-\mathfrak{q}_{i,1}\zeta_{i,1}^{1+\mathfrak{n}}-\mathfrak{r}_{i,1}z_{i,1}^{1+\mathfrak{n}}\right.$$
$$\left.-\mathfrak{q}_{i,2}\zeta_{i,2}^{1+\mathfrak{n}}-\mathfrak{r}_{i,2}z_{i,2}^{1+\mathfrak{n}}+\mathfrak{r}_{i,1}\zeta_{i,1}z_{i,1}^{\mathfrak{n}}+\mathfrak{r}_{i,2}\zeta_{i,2}z_{i,2}^{\mathfrak{n}}+\frac{\mathfrak{l}_{i,1}}{2\mathfrak{k}_{i,1}}(\Lambda_i^2-\tilde{\Lambda}_i^2)\right\}$$
$$+\sum_{i=1}^{3}\frac{\mathfrak{l}_{i,2}}{2\mathfrak{k}_{i,2}}(\Gamma_i^2-\tilde{\Gamma}_i^2)+\sum_{i=1}^{6}\left\{\frac{1}{2}\bar{d}_i^2+0.557g_i\rho_i\kappa_i+\frac{1}{2}\mathfrak{D}_i(\delta_i^{2\iota\sigma})\right\}$$
$$+\frac{1}{2}\sum_{i=1}^{3}(\mathfrak{h}_i^2+\bar{\omega}_i^2). \tag{33}$$

According to Lemma 3, the following inequalities can be obtained

$$\zeta_{i,j}z_{i,j}^{\mathfrak{n}}\leq\frac{1}{1+\mathfrak{n}}\mid\zeta_{i,j}\mid^{1+\mathfrak{n}}+\frac{\mathfrak{n}}{1+\mathfrak{n}}\mid z_{i,j}\mid^{1+\mathfrak{n}} \tag{34}$$

$$\left(\frac{1}{2\mathfrak{k}_{i,1}}\tilde{\Lambda}_i^2\right)^{\frac{1+\mathfrak{n}}{2}}\leq\frac{1}{4\mathfrak{k}_{i,1}}\tilde{\Lambda}_i^2+\frac{1-\mathfrak{n}}{2}(1+\mathfrak{n})^{\frac{1+\mathfrak{n}}{1-\mathfrak{n}}} \tag{35}$$

$$\left(\frac{1}{2\mathfrak{k}_{i,2}}\tilde{\Gamma}_i^2\right)^{\frac{1+\mathfrak{n}}{2}}\leq\frac{1}{4\mathfrak{k}_{i,2}}\tilde{\Gamma}_i^2+\frac{1-\mathfrak{n}}{2}(1+\mathfrak{n})^{\frac{1+\mathfrak{n}}{1-\mathfrak{n}}}. \tag{36}$$

Then, substituting (34)–(36) into (33) yields

$$\dot{V}_2 \leq \sum_{i=1}^{6}\left\{-\mathfrak{p}_{i,1}\zeta_{i,1}^2-(\mathfrak{p}_{i,1}-\frac{1}{2})z_{i,1}^2-\mathfrak{p}_{i,2}\zeta_{i,2}^2-\mathfrak{p}_{i,2}z_{i,2}^2-\frac{\mathfrak{l}_{i,1}}{4\mathfrak{k}_{i,1}}\tilde{\Lambda}_i^2\right.$$
$$-(\mathfrak{q}_{i,1}-\frac{\mathfrak{r}_{i,1}}{1+\mathfrak{n}})\zeta_{i,1}^{1+\mathfrak{n}}-\frac{\mathfrak{r}_{i,1}}{1+\mathfrak{n}}z_{i,1}^{1+\mathfrak{n}}-(\mathfrak{q}_{i,2}-\frac{\mathfrak{r}_{i,2}}{1+\mathfrak{n}})\zeta_{i,2}^{1+\mathfrak{n}}-\frac{\mathfrak{r}_{i,2}}{1+\mathfrak{n}}z_{i,2}^{1+\mathfrak{n}}$$
$$\left.-\mathfrak{l}_{i,1}(\frac{1}{2\mathfrak{k}_{i,1}}\tilde{\Lambda}_i^2)^{\frac{1+\mathfrak{n}}{2}}\right\}-\sum_{j=1}^{3}\left\{\frac{\mathfrak{l}_{j,2}}{4\mathfrak{k}_{j,2}}\tilde{\Gamma}_j^2+\mathfrak{l}_{j,2}(\frac{1}{2\mathfrak{k}_{j,2}}\tilde{\Gamma}_j^2)^{\frac{1+\mathfrak{n}}{2}}\right\}$$
$$+\sum_{i=1}^{6}\left\{\frac{\mathfrak{l}_{i,1}}{2\mathfrak{k}_{i,1}}\Lambda_i^2\right.$$
$$\left.+\mathfrak{l}_{i,1}\frac{1-\mathfrak{n}}{2}(1+\mathfrak{n})^{\frac{1+\mathfrak{n}}{1-\mathfrak{n}}}+\frac{1}{2}\bar{d}_i^2+0.557g_i\rho_i\kappa_i+\frac{1}{2}\mathfrak{D}_i(\delta_i^{2\iota\sigma})\right\}$$
$$+\sum_{j=1}^{3}\left\{\frac{\mathfrak{l}_{j,2}}{2\mathfrak{k}_{j,2}}\Gamma_j^2+\mathfrak{l}_{j,2}\frac{1-\mathfrak{n}}{2}(1+\mathfrak{n})^{\frac{1+\mathfrak{n}}{1-\mathfrak{n}}}\right\}+\frac{1}{2}\sum_{j=1}^{3}\left(\mathfrak{h}_j^2+\bar{\omega}_j^2\right). \tag{37}$$

Furthermore, the inequality (37) can be rewritten as

$$\dot{V}_2 \leq -\mathfrak{w}_1 V_2-\mathfrak{w}_2 V_2^{\frac{1+\mathfrak{n}}{2}}+\mathfrak{w}_3, \tag{38}$$

where $\mathfrak{w}_1=\min\left\{2\mathfrak{p}_{i,1},2(\mathfrak{p}_{i,1}-\frac{1}{2}),2\mathfrak{p}_{i,2},\frac{\mathfrak{l}_{i,1}}{2},\frac{\mathfrak{l}_{j,2}}{2}\right\}$, $\mathfrak{w}_2=\min\left\{2^{\frac{1+\mathfrak{n}}{2}}(\mathfrak{q}_{i,1}-\frac{\mathfrak{r}_{i,1}}{1+\mathfrak{n}}),2^{\frac{1+\mathfrak{n}}{2}}\frac{\mathfrak{r}_{i,1}}{1+\mathfrak{n}},2^{\frac{1+\mathfrak{n}}{2}}(\mathfrak{q}_{i,2}-\frac{\mathfrak{r}_{i,2}}{1+\mathfrak{n}}),2^{\frac{1+\mathfrak{n}}{2}}\frac{\mathfrak{r}_{i,2}}{1+\mathfrak{n}},\right.$ $\left.\mathfrak{l}_{i,1},\mathfrak{l}_{j,2}\right\}$, and $\mathfrak{w}_3=\sum_{i=1}^{6}\left\{\frac{\mathfrak{l}_{i,1}}{2\mathfrak{k}_{i,1}}\Lambda_i^2+\mathfrak{l}_{i,1}\frac{1-\mathfrak{n}}{2}(1+\mathfrak{n})^{\frac{1+\mathfrak{n}}{1-\mathfrak{n}}}+\frac{1}{2}\bar{d}_i^2+\right.$ $\left.0.557g_i\rho_i\kappa_i+\frac{1}{2}\mathfrak{D}_i(\delta_i^{2\iota\sigma})\right\}+\frac{1}{2}\sum_{j=1}^{3}\left\{\mathfrak{h}_j^2+\bar{\omega}_j^2\right\}+\sum_{j=1}^{3}$ $\left\{\frac{\mathfrak{l}_{j,2}}{2\mathfrak{k}_{j,2}}\Gamma_j^2+\mathfrak{l}_{j,2}\frac{1-\mathfrak{n}}{2}(1+\mathfrak{n})^{\frac{1+\mathfrak{n}}{1-\mathfrak{n}}}\right\}$. From (38), we consider the following two cases.

Case 1. For $0<\pi_0<1$, $\dot{V}_2\leq-\pi_0\mathfrak{w}_1 V_2-(1-\pi_0)\mathfrak{w}_1 V_2-\mathfrak{w}_2 V_2^{\frac{1+\mathfrak{n}}{2}}+\mathfrak{w}_3$. If $V_2>\mathfrak{w}_3/((1-\pi_0)\mathfrak{w}_1)$,

it can be derived that $\dot{V}_2\leq-\pi_0\mathfrak{w}_1 V_2-\mathfrak{w}_2 V_2^{\frac{1+\mathfrak{n}}{2}}$. According to Lemma 1, one has

$$\left(\zeta_{i,1},z_{i,1},\zeta_{i,2},z_{i,2},\tilde{\Lambda}_i,\tilde{\Gamma}_j\right)\in\left\{V_2\leq\frac{\mathfrak{w}_3}{(1-\pi_0)\mathfrak{w}_1}\right\}$$

within the finite time

$$t_1^*\leq\frac{2}{\pi_0\mathfrak{w}_1(1-\mathfrak{n})}\ln\frac{\pi_0\mathfrak{w}_1 V_2^{\frac{1-\mathfrak{n}}{2}}(t_0)+\mathfrak{w}_2}{\mathfrak{w}_2}.$$

Case 2. $\dot{V}_2\leq-\mathfrak{w}_1 V_2-\pi_0\mathfrak{w}_2 V_2^{\frac{1+\mathfrak{n}}{2}}-(1-\pi_0)\mathfrak{w}_2 V_2^{\frac{1+\mathfrak{n}}{2}}+\mathfrak{w}_3$, where $0<\pi_0<1$. $\dot{V}_2\leq-\mathfrak{w}_1 V_2-\pi_0\mathfrak{w}_2 V_2^{\frac{1+\mathfrak{n}}{2}}$ is obtained when $V_2^{\frac{1+\mathfrak{n}}{2}}>\mathfrak{w}_3/((1-\pi_0)\mathfrak{w}_2)$. In the same way, it can be achieved that

$$\left(\zeta_{i,1},z_{i,1},\zeta_{i,2},z_{i,2},\tilde{\Lambda}_i,\tilde{\Gamma}_j\right)\in\left\{V_2\leq\left(\frac{\mathfrak{w}_3}{(1-\pi_0)\mathfrak{w}_2}\right)^{\frac{2}{1+\mathfrak{n}}}\right\}$$

in a finite time

$$t_2^*\leq\frac{2}{\mathfrak{w}_1(1-\mathfrak{n})}\ln\frac{\mathfrak{w}_1 V_2^{\frac{1-\mathfrak{n}}{2}}(t_0)+\pi_0\mathfrak{w}_2}{\pi_0\mathfrak{w}_2}.$$

From the discussion of the above two cases, it can be further obtained that the finite-time boundedness of all signals $\zeta_{i,1}$, $z_{i,1}$, $\zeta_{i,2}$, $z_{i,2}$, $\tilde{\Lambda}_i$, and $\tilde{\Gamma}_j$ in the closed-loop system. Namely, $\zeta_{i,1}$ and $z_{i,1}$ will converge into the region

$$\mid\zeta_{i,1}\mid\leq\min\left\{\sqrt{\frac{2\mathfrak{w}_3}{(1-\pi_0)\mathfrak{w}_1}},\sqrt{2\left(\frac{\mathfrak{w}_3}{(1-\pi_0)\mathfrak{w}_2}\right)^{\frac{2}{1+\mathfrak{n}}}}\right\}$$

$$\mid z_{i,1}\mid\leq\min\left\{\sqrt{\frac{2\mathfrak{w}_3}{(1-\pi_0)\mathfrak{w}_1}},\sqrt{2\left(\frac{\mathfrak{w}_3}{(1-\pi_0)\mathfrak{w}_2}\right)^{\frac{2}{1+\mathfrak{n}}}}\right\}$$

in a finite time

$$t_3^*=\max\left\{\frac{2}{(\pi_0\mathfrak{w}_1(1-\mathfrak{n}))}\ln\frac{\pi_0\mathfrak{w}_1 V_2^{\frac{1-\mathfrak{n}}{2}}(t_0)+\mathfrak{w}_2}{\mathfrak{w}_2},\right.$$
$$\left.\frac{2}{\mathfrak{w}_1(1-\mathfrak{n})}\ln\frac{\mathfrak{w}_1 V_2^{\frac{1-\mathfrak{n}}{2}}(t_0)+\pi_0\mathfrak{w}_2}{\pi_0\mathfrak{w}_2}\right\}.$$

For $t\geq t_3^*$, $v_{i,1}$ reaches the following region

$$v_{i,1}\leq\min\left\{2\sqrt{\frac{2\mathfrak{w}_3}{(1-\pi_0)\mathfrak{w}_1}},2\sqrt{2\left(\frac{\mathfrak{w}_3}{(1-\pi_0)\mathfrak{w}_2}\right)^{\frac{2}{1+\mathfrak{n}}}}\right\}.$$

Obviously, the tracking errors of attitude and position subsystems can be regulated to a sufficient neighborhood around origin in a finite time t_3^* through the selection of appropriate control design parameters.

Notice that for the definitions in (16) and (27), for arbitrary positive integer k, there exists $t^* > 0$ such that $t_{k+1,i} - t_{k,i} \le t^*$. To this end, by recalling $e_i(t) = \beta_i(t) - u_i^a(t)$, $t \in [t_{k,i}, t_{k+1,i})$, one has $d|e_i|/dt = \text{sign}(e_i)\dot{e}_i \le |\dot{\beta}_i|$. Furthermore, by substituting (15) and (25) into (17) and (28), one has

$$\dot{\beta}_i = -(1 + \mu_i)\left(\dot{\alpha}_{i,2}\tanh\left(\frac{\zeta_{i,2}\alpha_{i,2}}{\kappa_i}\right) + \frac{\alpha_{i,2}}{\kappa_i}\frac{\dot{\zeta}_{i,2}\bar{\beta}_i + \zeta_{i,2}\dot{\alpha}_{i,2}}{\cosh^2\left(\frac{\zeta_{i,2}\alpha_{i,2}}{\kappa_i}\right)}\right)$$
$$+ \frac{\varsigma_{i,1}}{\kappa_i}\frac{\dot{\zeta}_{i,2}\varsigma_{i,1}}{\cosh^2\left(\frac{\zeta_{i,2}\varsigma_{i,1}}{\kappa_i}\right)},$$

(39)

where $\bar{\beta}_i$ is the upper bound of $|\dot{\beta}_i|$. Then it can be derived that $\dot{\beta}_i$ is bounded and the Zeno behavior can be successfully avoided. $\square$

Remark 2 The radius of region for attitude and position tracking errors are closely related to the designed parameters $\mathfrak{p}_{i,j}$, $\mathfrak{q}_{i,j}$, $\mathfrak{r}_{i,j}$, $\mathfrak{h}_i$, $\mathfrak{f}_{i,j}$, and $\mathfrak{l}_{i,j}$. The larger parameters $\mathfrak{p}_{i,j}$, $\mathfrak{q}_{i,j}$, and $\mathfrak{f}_{i,j}$ and the smaller parameters $\mathfrak{r}_{i,j}$, $\mathfrak{h}_i$, and $\mathfrak{l}_{i,j}$ can enable the faster setting time and smaller convergence region.

5 Simulation Results

In this section, the comparison simulations are implemented to show the effectiveness of the developed fuzzy approximation-based event-triggered adaptive finite-time fault-tolerant control algorithm. The physical parameters of quadrotor UAV are listed in Table 1.

The parameters of actuator faults are given as $\rho_i = 0.8$. When $t \ge 8$, $b_1 = 5\sin t$, $b_2 = 3\cos t$, and $b_3 = 4\cos(2t)$, and when $t \ge 10$, $b_4 = 5\cos(0.5t)$, $b_5 = 4\sin t$, and $b_6 = 3\sin(2t)$. The reference trajectories are given as $[\eta_3^d, \eta_4^d, \eta_5^d, \eta_6^d] = [0, t/8, \sin(\pi t/9), \cos(\pi t/9)]$. In the simulations, the initial conditions are set as $[\eta_1, \eta_2, \eta_3, \eta_4, \eta_5, \eta_6] = [0, 0, \pi/4, 1, 1, 0]$. The control

Table 1 The physical parameters of quadrotor UAV

Parameter	Value	Parameter	Value
a	0.2 m	I_z	0.96 kg m^2
m	2 kg	J_r	0.01 kg m^2
g	9.8 m/s^2	d_1	$\sin(\pi t/5)$
G_ϕ	0.6 kg/rad	d_2	$\cos(\pi t/6)$
G_θ	0.6 kg/rad	d_3	$\sin(\pi t/7)$
G_ψ	0.6 kg/rad	d_4	$\cos(\pi t/7)$
I_x	0.55 kg m^2	d_5	$\sin(\pi t/8)$
I_y	0.51 kg m^2	d_6	$\sin(\pi t/9)$

design parameters are chosen as $\mathfrak{K}_i = 0.01$, $\mathfrak{L}_{i,1} = 8$, and $\mathfrak{L}_{i,2} = 5$; $\mathfrak{p}_{i,1} = 2$, $\mathfrak{p}_{i,2} = 3$, $\mathfrak{q}_{i,1} = \mathfrak{r}_{i,1} = 3$, $\mathfrak{q}_{i,2} = \mathfrak{r}_{i,2} = 4$, $\mathfrak{f}_{i,1} = \mathfrak{f}_{i,2} = 2$, $\mathfrak{l}_{i,1} = 3$, $\mathfrak{l}_{i,2} = 5$, and $\mathfrak{h}_i = 0.1$; $\mu_i = 0.5$, $\kappa_i = 10$, $\varsigma_{i,1} = 5$, $\varsigma_{1,2} = \varsigma_{2,2} = \varsigma_{3,2} = 2$, and $\varsigma_{4,2} = \varsigma_{5,2} = \varsigma_{6,2} = 1$.

The simulation results are shown in Figs. 2, 3, 4, 5, 6, and 7. The curves of the attitude and position outputs η_i and the reference trajectories η_i^d are depicted in Fig. 2. The curves of parameter tuning laws $\hat{\Gamma}_i$ are plotted in Fig. 3. The curves of event-triggered control laws u_i^a and its triggering time intervals of control inputs for attitude and position subsystems are revealed in Figs. 4, 5, 6, and 7, respectively. Moreover, the data of control signal transmission times of the time-triggered control (TTC) algorithm and ETC algorithm are given in Table 2. It can be observed that the outputs of attitude and position subsystems can still precisely track the reference trajectories even suffer from actuator faults. The execution number of actuators is reduced without significantly reducing system performance.

Remark 3 The trial-and-error method for adjusting control design parameters is implemented for better control action and tracking performance. Nevertheless, there is still a deficiency of many design parameters, which will be improved in future based on learning and optimal approaches [53, 54].

At last, the comparison simulations with the FTCFB, CFB, and DSC are performed to demonstrate the superiority of the proposed algorithm. The control design parameters for CFB algorithm and DSC algorithm are identical to the FTCFB algorithm. The simulation results are shown in Fig. 8, with which the modified attitude and position tracking errors $\upsilon_{i,1} = \eta_i - \eta_i^d$ are applied to evaluate the performance of three algorithms. It can be observed that the proposed event-triggered-based FTCFB control algorithm can achieve the desired performance with a smaller tracking error and a faster convergence rate.

6 Conclusion

In this article, the problem of event-triggered adaptive finite-time fault-tolerant control for a quadrotor UAV has been considered. By combining finite-time command filter and fractional power error compensation mechanism into the framework of backstepping design method, the issue of "explosion of complexity" and the effect of filtered error have been skillfully solved. The proposed event-triggered-based fault-tolerant control scheme has decreased the communication resources in spite of the quadrotor UAV suffering from actuator faults. It has been proven that the
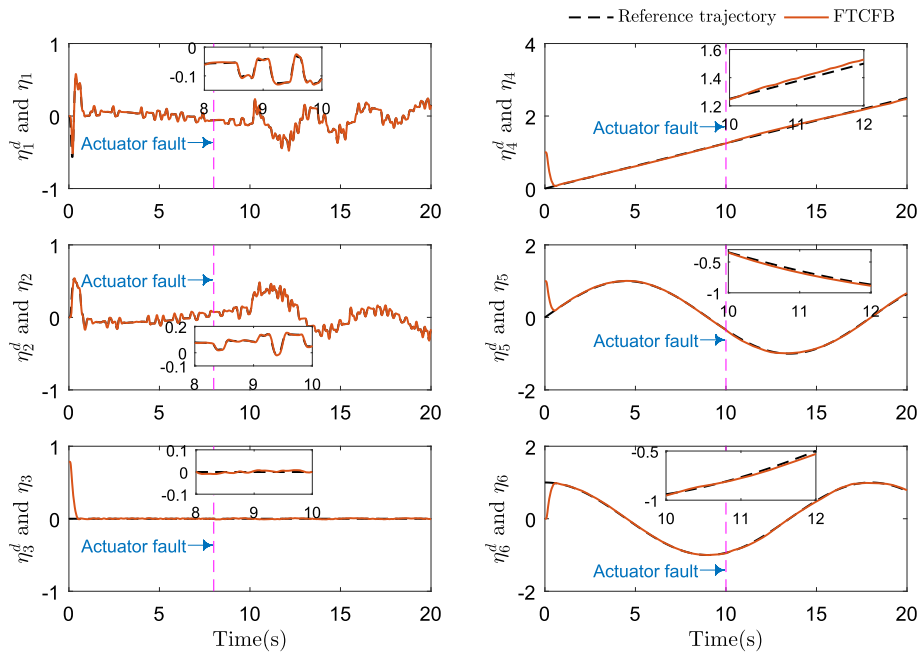
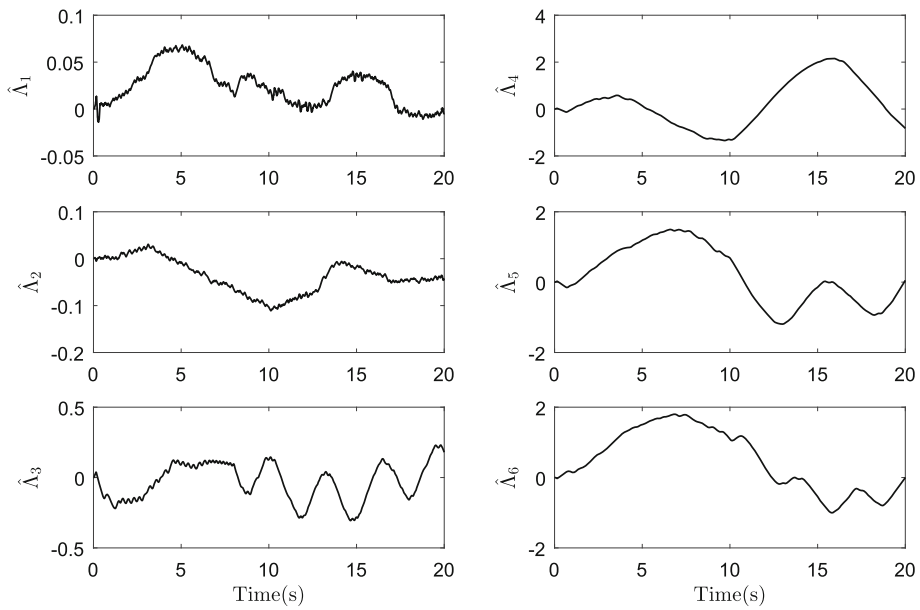Fig. 2 The curves of reference trajectories and system outputs

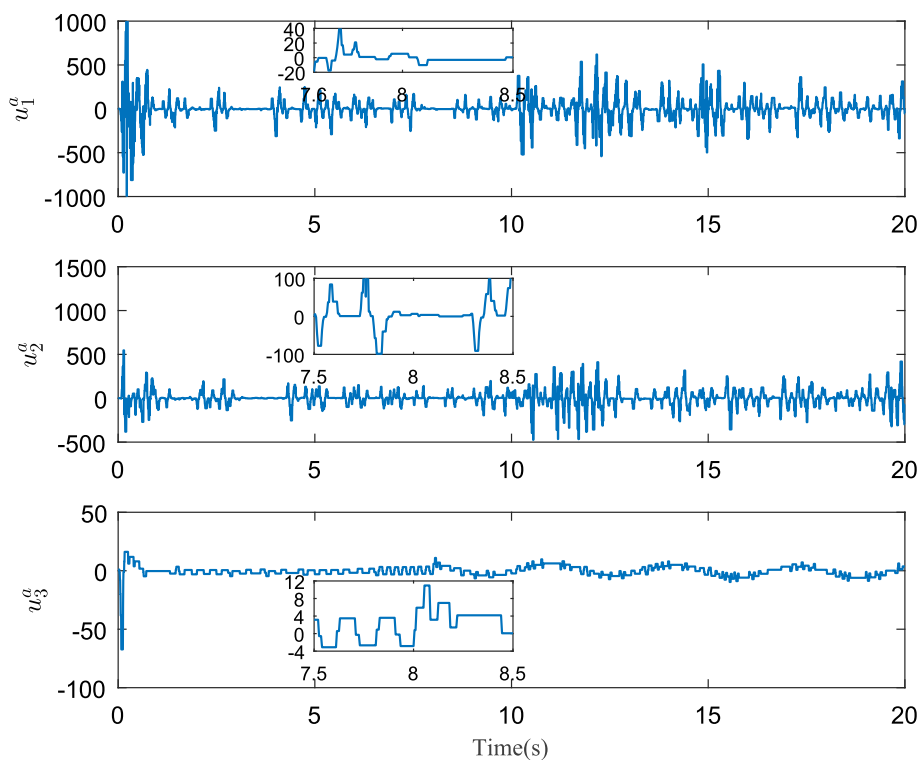Fig. 3 The curves of parameter tuning laws $\hat{\Lambda}_i$

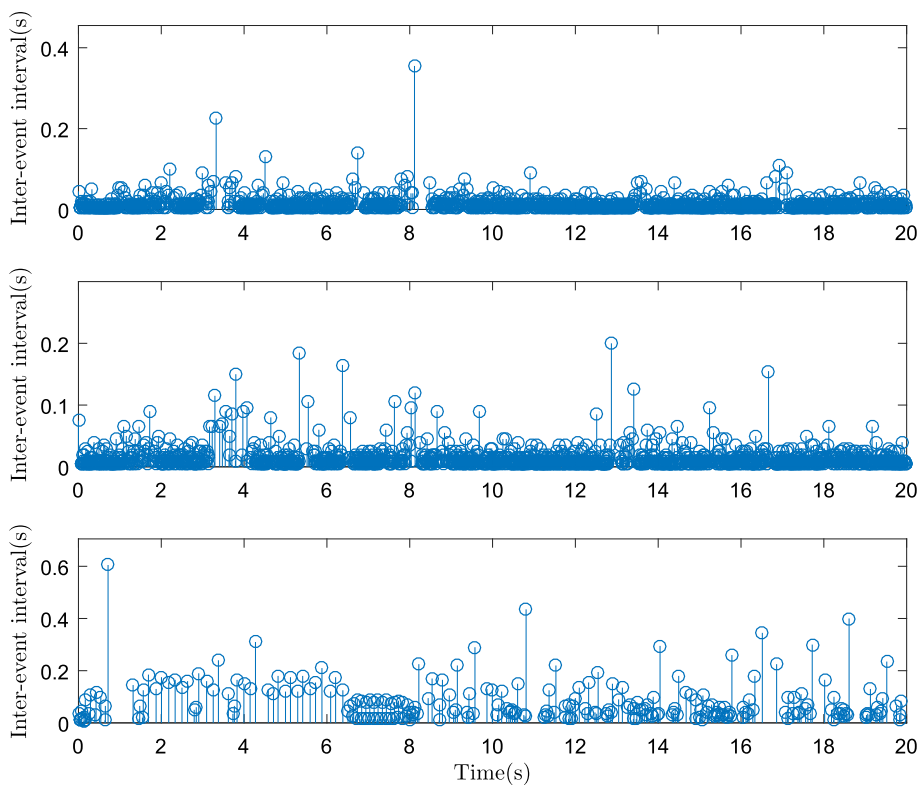**Fig. 4** The curves of event-triggered control laws of attitude subsystem

Fig. 5 The curves of the triggering interval of attitude control laws
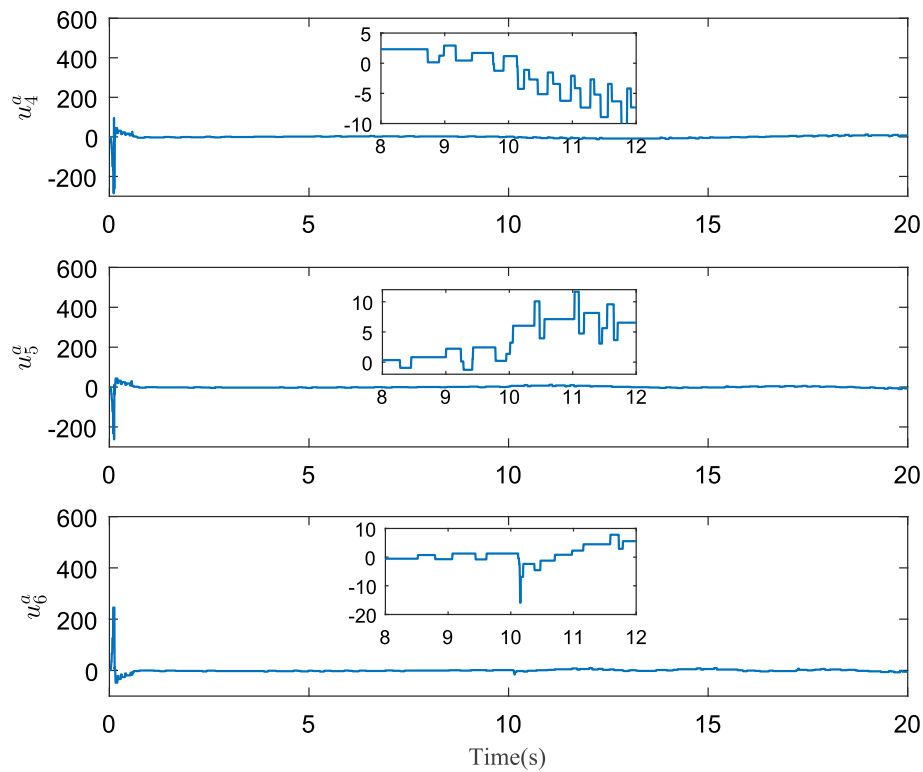
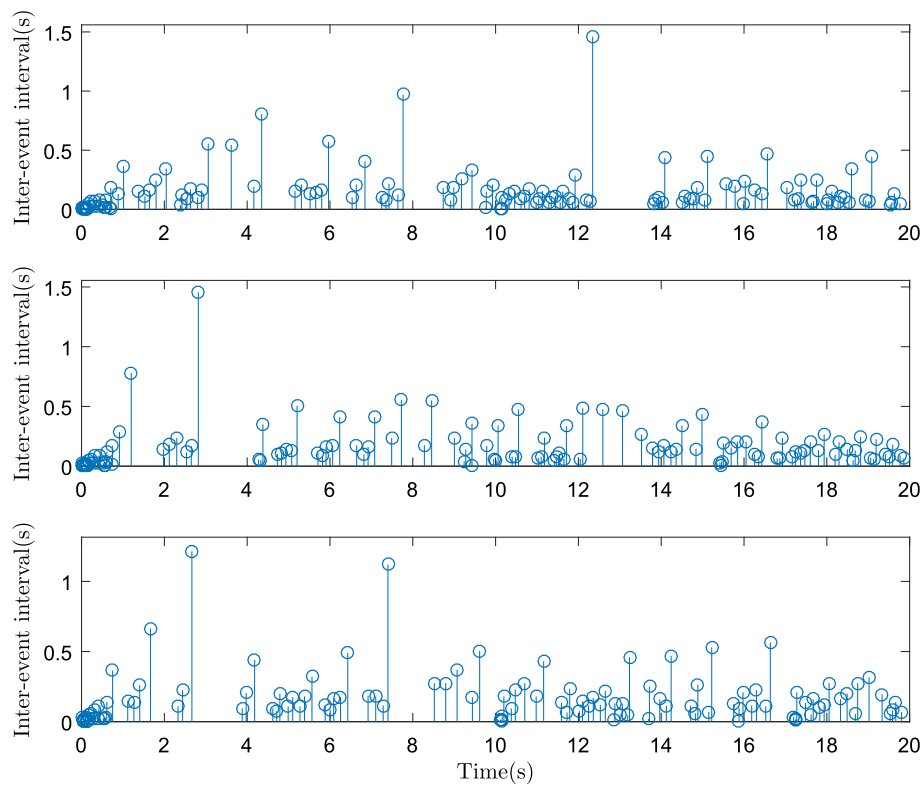**Fig. 6** The curves of event-triggered control laws of position subsystem

Fig. 7 The curves of the triggering interval of position control laws

Table 2 The comparison of the TTC algorithm and ETC algorithm in data transmission

Control method	The number of transmission data					
	u_1^a	u_2^a	u_3^a	u_4^a	u_5^a	u_6^a
TTC algorithm	4000	4000	4000	4000	4000	4000
ETC algorithm	1712	1636	367	271	246	260
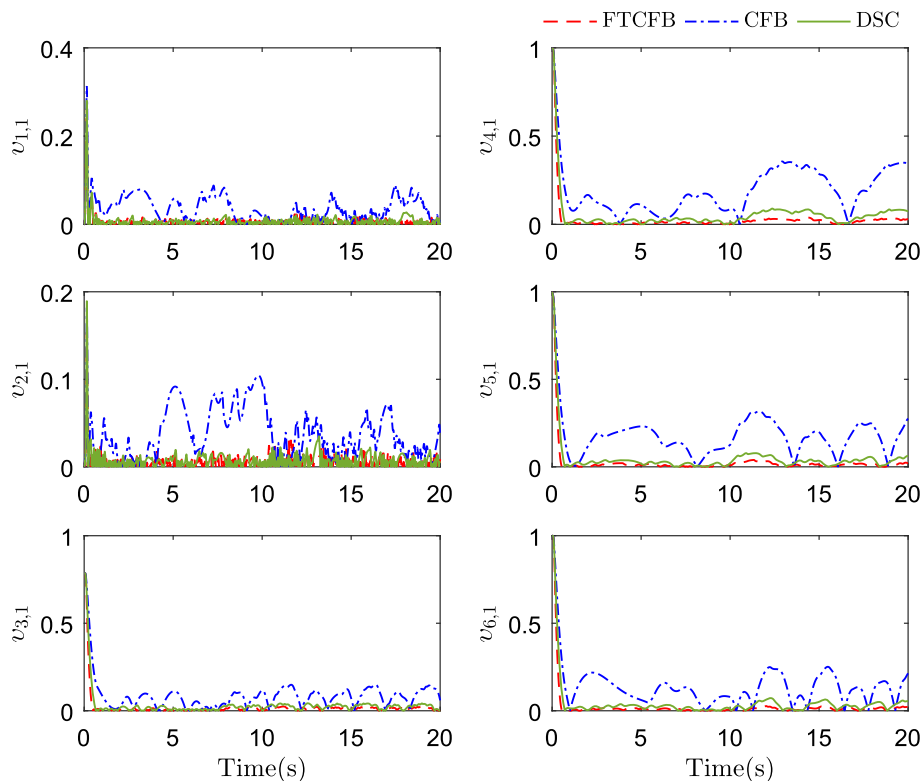
Fig. 8 The curves of attitude and position tracking errors under different control schemes

tracking errors of the attitude and position subsystems approach to a small neighborhood near the origin in a finite time. In future study, the fuzzy approximation-based event-triggered adaptive finite-time output feedback control for the quadrotor UAV will be considered.

References

1. Dierks, T., Jagannathan, S.: Output feedback control of a quadrotor UAV using neural networks. IEEE Trans. Neural Netw. **21**(1), 50–66 (2009)

2. Xian, B., Guo, J., Zhang, Y.: Adaptive backstepping tracking control of a 6-dof unmanned helicopter. IEEE/CAA J. Autom. Sin. **2**(1), 19–24 (2015)

3. Liu, H., Li, D., Zuo, Z., Zhong, Y.: Robust three-loop trajectory tracking control for quadrotors with multiple uncertainties. IEEE Trans. Ind. Electron. **63**(4), 2263–2274 (2016)

4. Shao, S., Chen, M.: Adaptive neural discrete-time fractional-order control for a UAV system with prescribed performance using disturbance observer. IEEE Trans. Syst. Man Cybern.: Syst. **51**(2), 742–754 (2021)

5. Seyedtabaii, S.: New flat phase margin fractional order pid design: Perturbed UAV roll control study. Robot. Auton. Syst. **96**, 58–64 (2017)

6. Zheng, E., Xiong, J., Luo, J.: Second order sliding mode control for a quadrotor UAV. ISA Trans. **53**(4), 1350–1356 (2014)

7. Wang, B., Zhang, Y.: An adaptive fault-tolerant sliding mode control allocation scheme for multirotor helicopter subject to simultaneous actuator faults. IEEE Trans. Ind. Electron. **65**(5), 4227–4236 (2017)

8. Wang, R., Liu, J.: Trajectory tracking control of a 6-DOF quadrotor UAV with input saturation via backstepping. J. Frankl. Inst. **355**(7), 3288–3309 (2018)

9. Yu, G., Cabecinhas, D., Cunha, R., Silvestre, C.: Nonlinear backstepping control of a quadrotor-slung load system. IEEE/ASME Trans. Mechatron. **24**(5), 2304–2315 (2019)

10. Xie, W., Cabecinhas, D., Cunha, R., Silvestre, C.: Adaptive backstepping control of a quadcopter with uncertain vehicle mass, moment of inertia, and disturbances. IEEE Trans. Ind. Electron. **69**(1), 549–559 (2022)

11. Shao, X., Liu, J., Cao, H., Shen, C., Wang, H.: Robust dynamic surface trajectory tracking control for a quadrotor UAV via extended state observer. Int. J. Robust Nonlinear Control **28**(7), 2700–2719 (2018)

12. Shen, Z., Li, F., Cao, X., Guo, C.: Prescribed performance dynamic surface control for trajectory tracking of quadrotor uav with uncertainties and input constraints. Int. J. Control **94**(11), 2945–2955 (2021)

13. Wu, X., Zheng, W., Zhou, X., Shao, S.: Adaptive dynamic surface and sliding mode tracking control for uncertain QUAV with time-varying load and appointed-time prescribed performance. J. Frankl. Inst. **358**(8), 4178–4208 (2021)

14. Aboudonia, A., El-Badawy, A., Rashad, R.: Active anti-disturbance control of a quadrotor unmanned aerial vehicle using the command-filtering backstepping approach. Nonlinear Dyn. **90**, 581–597 (2017)

15. Cao, L., Wang, Y., Zhang, S., Fei, T.: Command-filtered sensor-based backstepping controller for small unmanned aerial vehicles with actuator dynamics. Int. J. Syst. Sci. **49**(16), 3365–3376 (2018)

16. Liu, K., Wang, R.: Antisaturation command filtered backstepping control based disturbance rejection for a quadarotor UAV. IEEE Trans. Circuits Syst. II: Express Briefs **68**(12), 3577–3581 (2021)

17. Sofianos, N.A., Boutalis, Y.S.: Robust adaptive multiple models based fuzzy control of nonlinear systems. Neurocomputing **173**, 1733–1742 (2016)

18. Zhou, Q., Li, H., Wu, C., Wang, L., Ahn, C.K.: Adaptive fuzzy control of nonlinear systems with unmodeled dynamics and input saturation using small-gain approach. IEEE Trans. Syst. Man Cybern.: Syst. **47**(8), 1979–1989 (2017)

19. Fan, X., Bai, P., Li, H., Deng, X., Lv, M.: Adaptive fuzzy finite-time tracking control of uncertain non-affine multi-agent systems with input quantization. IEEE Access **8**, 187623–187633 (2020)

20. Song, S., Park, J.H., Zhang, B., Song, X.: Event-based adaptive fuzzy fixed-time secure control for nonlinear CPSs against unknown false data injection and backlash-like hysteresis. IEEE Trans. Fuzzy Syst. **30**(6), 1939–1951 (2022)

21. Su, H., Hu, Y., Karimi, H.R., Knoll, A., Ferrigno, G., De Momi, E.: Improved recurrent neural network-based manipulator control with remote center of motion constraints: Experimental results. Neural Netw. **131**, 291–299 (2020)

22. Su, H., Qi, W., Hu, Y., Karimi, H.R., Ferrigno, G., De Momi, E.: An incremental learning framework for human-like redundancy optimization of anthropomorphic manipulators. IEEE Trans. Ind. Inform. **18**(3), 1864–1872 (2022)

23. Song, S., Park, J.H., Zhang, B., Song, X.: Adaptive NN finite-time resilient control for nonlinear time-delay systems with unknown false data injection and actuator faults. IEEE Trans. Neural Netw. Learn. Syst. (2021). https://doi.org/10.1109/TNNLS.2021.3070623

24. Tran, V.P., Santoso, F., Garratt, M.A., Petersen, I.R.: Adaptive second-order strictly negative imaginary controllers based on the interval type-2 fuzzy self-tuning systems for a hovering quadrotor with uncertainties. IEEE/ASME Trans. Mechatron. **25**(1), 11–20 (2020)

25. Hua, C., Jiang, A., Li, K.: Adaptive neural network finite-time tracking quantized control for uncertain nonlinear systems with full-state constraints and applications to QUAVs. Neurocomputing **440**(14), 264–274 (2021)

26. Zhang, X., Wang, Y., Zhu, G., Chen, X., Li, Z., Wang, C., Su, C.Y.: Compound adaptive fuzzy quantized control for quadrotor and its experimental verification. IEEE Trans. Cybern. **51**(3), 1121–1133 (2021)

27. Wang, J., Wang, P., Ma, X.: Adaptive event-triggered control for quadrotor aircraft with output constraints. Aerosp. Sci. Technol. **105**, 105935 (2020)

28. Zhu, X.Z., Casau, P., Silvestre, C.: Event-triggered global trajectory tracking control of a quadrotor: synthesis, simulations, and experiments. Int. J. Robust Nonlinear Control **31**(13), 6144–6165 (2021)

29. Tian, B., Cui, J., Lu, H., Liu, L., Zong, Q.: Attitude control of uavs based on event-triggered supertwisting algorithm. IEEE Trans. Ind. Inform. **17**(2), 1029–1038 (2021)

30. Lin, X., Liu, J., Yu, Y., Sun, C.: Event-triggered reinforcement learning control for the quadrotor UAV with actuator saturation. Neurocomputing **415**, 135–145 (2020)

31. Shao, S., Chen, M., Hou, J., Zhao, Q.: Event-triggered-based discrete-time neural control for a quadrotor UAV using disturbance observer. IEEE/ASME Trans. Mechatron. **26**(2), 689–699 (2021)

32. Wang, H., Kang, S., Feng, Z.: Finite-time adaptive fuzzy command filtered backstepping control for a class of nonlinear systems. Int. J. Fuzzy Syst. **21**, 2575–2587 (2019)

33. Diao, S., Sun, W., Wang, L., Wu, J.: Finite-time adaptive fuzzy control for nonlinear systems with unknown backlash-like hysteresis. Int. J. Fuzzy Syst. **23**, 2037–2047 (2021)

34. Du, H., Zhu, W., Wen, G., Wu, D.: Finite-time formation control for a group of quadrotor aircraft. Aerosp. Sci. Technol. **69**, 609–616 (2017)

35. Tian, B., Cui, J., Lu, H., Zuo, Z., Zong, Q.: Adaptive finite-time attitude tracking of quadrotors with experiments and comparisons. IEEE Trans. Ind. Electron. **66**(12), 9428–9438 (2019)

36. Chen, Q., Ye, Y., Hu, Z., Na, J., Wang, S.: Finite-time approximation-free attitude control of quadrotors: theory and experiments. IEEE Trans. Aerosp. Electron. Syst. **57**(3), 1780–1792 (2021)

37. Eliker, K., Grouni, S., Tadjine, M., Zhang, W.: Practical finite time adaptive robust flight control system for quad-copter UAVs. Aerosp. Sci. Technol. **98**, 105708 (2020)

38. Mofid, O., Mobayen, S.: Adaptive finite-time back-stepping global sliding mode tracker of quad-rotor UAVs under model uncertainty, wind perturbation and input saturation. IEEE Trans. Aerosp. Electron. Syst. (2021). https://doi.org/10.1109/TAES.2021.3098168

39. Lanzon, A., Freddi, A., Longhi, S.: Flight control of a quadrotor vehicle subsequent to a rotor failure. J. Guid. Control Dyn. **37**(2), 580–591 (2014)

40. Chen, F., Jiang, R., Zhang, K., Jiang, B., Tao, G.: Robust backstepping sliding-mode control and observer-based fault estimation for a quadrotor UAV. IEEE Trans. Ind. Electron. **63**(8), 5044–5056 (2016)

41. Hao, W., Xian, B.: Nonlinear adaptive fault-tolerant control for a quadrotor UAV based on immersion and invariance methodology. Nonlinear Dyn. **90**, 2813–2826 (2017)

42. Yu, Z., Liu, Z., Zhang, Y., Qu, Y., Su, C.Y.: Distributed finite-time fault-tolerant containment control for multiple unmanned aerial vehicles. IEEE Trans. Neural Netw. Learn. Syst. **31**(6), 2077–2091 (2020)

43. Liu, K., Wang, R., Wang, X., Wang, X.: Anti-saturation adaptive finite-time neural network based fault-tolerant tracking control

for a quadrotor UAV with external disturbances. Aerosp. Sci. Technol. **115**, 106790 (2021)

44. Yu, Z., Zhang, Y., Liu, Z., Qu, Y., Su, C.Y., Jiang, B.: Decentralized finite-time adaptive fault-tolerant synchronization tracking control for multiple UAVs with prescribed performance. J. Frankl. Inst. **357**(16), 11830–11862 (2020)
45. Li, Y., Ma, Z., Tong, S.: Adaptive fuzzy fault-tolerant control of nontriangular structure nonlinear systems with error constraint. IEEE Trans. Fuzzy Syst. **26**(4), 2062–2074 (2018)
46. Wang, L.: Adaptive fuzzy systems and control: design and stability analysis. Prentice-Hall, Englewood Cliffs (1994)
47. Wang, F., Chen, B., Lin, C., Zhang, J., Meng, X.: Adaptive neural network finite-time output feedback control of quantized nonlinear systems. IEEE Trans. Cybern. **48**(6), 1839–1848 (2017)
48. Yu, J., Shi, P., Zhao, L.: Finite-time command filtered backstepping control for a class of nonlinear systems. Automatica **92**, 173–180 (2018)
49. Qian, C., Lin, W.: A continuous feedback approach to global strong stabilization of nonlinear systems. IEEE Trans. Autom. Control **46**(7), 1061–1079 (2001)
50. Hardy, G.H., Littlewood, J.E., Pólya, G., Pólya, G., Littlewood, D.: Inequalities. Cambridge University Press, Cambridge (1952)
51. Cui, G., Yu, J., Wang, Q.G.: Finite-time adaptive fuzzy control for mimo nonlinear systems with input saturation via improved command-filtered backstepping. IEEE Trans. Syst. Man Cybern.: Syst. **52**(2), 980–989 (2022)
52. Wang, X., Chen, Z., Yang, G.: Finite-time-convergent differentiator based on singular perturbation technique. IEEE Trans. Autom.Control **52**(9), 1731–1737 (2007)
53. Qi, W., Aliverti, A.: A multimodal wearable system for continuous and real-time breathing pattern monitoring during daily activity. IEEE J. Biomed. Health Inform. **24**(8), 2199–2207 (2020)
54. Qi, W., Ovur, S.E., Li, Z., Marzullo, A., Song, R.: Multi-sensor guided hand gesture recognition for a teleoperated robot using a recurrent neural network. IEEE Robot. Autom. Lett. **6**(3), 6039–6045 (2021)

Wei Yang received the M.Sc. degree from Suzhou University of Science and Technology, Suzhou, China, in 2022. He is currently pursuing the Ph.D. degree with the School of Automation, Qingdao University. His research interests include adaptive control and intelligent control for quadrotor UAV.

Guozeng Cui received the B.Sc. degree in applied mathematics from Shandong University of Technology, Zibo, China, in 2009, the M.Sc. degree in applied mathematics from Qufu Normal University, Qufu, China, in 2012, and the Ph.D. degree in control science and engineering from the Nanjing University of Science and Technology, Nanjing, China, in 2016. He is currently an Associate Professor with the School of Electronic and Information Engineering, Suzhou University of Science and Technology. His research interests include adaptive control, intelligent control for nonlinear systems, and multi-agent systems.
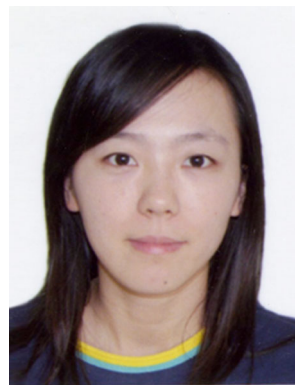
Ze Li received the B.Sc. degree in electronic information engineering from Nanjing University of Science and Technology, Nanjing, China, in 2005, and the Ph.D. degree in control science and engineering from Nanjing University of Science and Technology, Nanjing, China, in 2010. She is currently an Associate Professor with the School of Electronic and Information Engineering, Suzhou University of Science and Technology. Her research interests include robust control and filtering, time-delay systems, stochastic systems, nonlinear systems, and fuzzy systems.

Chongben Tao received the B.Sc. degree in electronic information engineering from Jiangnan University, Wuxi, China, in 2008, and the Ph.D. degree in control science and engineering from the Jiangnan University, Wuxi, China, in 2014. He is currently an Associate Professor with the School of Electronic and Information Engineering, Suzhou University of Science and Technology. His research interests include deep reinforcement learning, intelligent control for quadrotor UAV, and biped robot.